PNAS
www.pnas.org

Supplementary Information for

Allosteric Modulation of a Human Protein Kinase with Monobodies

Adelajda Zorba*, Vy Nguyen*, Akiko Koide, Marc Hoemberger, Yuejiao Zheng, Steffen Kutter, Chansik Kim, Shohei Koide[#] and Dorothee Kern[#]

* These authors contributed equally to this work

corresponding authors:

Email:
dkern@brandeis.edu and Shohei.Koide@nyulangone.org

This PDF file includes:

Supplementary text
Figs. S1 to S6
References for SI reference citations

www.pnas.org/cgi/doi/10.1073/pnas.1906024116

Supplementary text: MATERIALS AND METHODS

Monobody selection and affinity measurement

The monobody libraries have been described previously [1]. We used the selection method described in [1-3] with minor modifications. A flow chart of the selection design is shown in **SI Appendix Fig. 1A.** A total of four rounds of phage selection were performed. In the second, third and fourth rounds, amplified phage particles were first incubated with streptavidin (SAV) magnetic beads (Promega) that had been complexed with biotinylated AurA-TPX2 fusion protein for 30 min. The concentrations of the SAV/Aurora A-TPX2 complexes were 4 μM (the second round), 2 μM (the third round) and 670 nM (the fourth round). Unbound phage particles were collected and used for selection for binding to biotinylated AurA at concentrations of 100, 100, 100 and 50 nM for rounds 1, 2, 3 and 4, respectively.

A yeast-display library was constructed using the recovered clones from the fourth round of phage-display selection, as described previously [1]. The first round of yeast-display library sorting was performed using 50 nM biotinylated AurA. Two additional rounds of negative sorting were performed with 500 nM AurA-TPX2 fusion in the first and with either 2 μM of AurA-Y199K mutant or AurA-Y199H mutant in the second. Monobody clones exhibiting the ratio of binding signal (defined as the median fluorescence signal of target binding of the entire monobody-displaying population in the yeast display format) to 2 μM mutant Aurora A (either Y199H or Y199K) over that to 0.27 μM wild type Aurora A of less than 0.2 were selected for further characterization.

The buffer used for phage-display selection was 20 mM TrisHCl pH 7.5, 200 mM NaCl, 20 mM $MgCl_2$, 0.5 mM TCEP and 0.5 mg/mL BSA. For yeast display the BSA concentration was increased to 1 mg/mL. Affinity measurements using the yeast display method have been described [1]. We have validated using numerous monobodies that K_d values measured in this manner are consistent with those determined from biophysical methods using purified monobodies [1, 4].

Expression and purification of AurA kinase, TPX2 and monobodies

TEV-cleavable, His_6-tagged dephosphorylated AurA kinase was obtained through a Lambda Protein Phosphatase co-expression system and purified as described in detail in [5].

His_6-tagged, GB1-tagged and thrombin cleavable $TPX2^{1-45}$ was transformed in BL21(DE3) cells and plated on Kanamycin TB plates. The most robust colony was used to inoculate a 1L TB culture to an OD = 0.2 and induced at an OD = 0.6-0.8 with 0.6 mM IPTG for 3 hours at 37 °C. Cells were centrifuged, resuspended in binding buffer (50 mM TrisHCl, 300 mM NaCl, 20 mM $MgCl_2$, pH 8.0), and sonicated in the presence of EDTA-free protease inhibitor cocktail and DNase. Lysates thus obtained were filtered using a 0.22 μm filtering unit and passed through a NiNTA column. Bound protein was thrombin cleaved overnight in a dialysis cassette in gel filtration buffer (20 mM TrisHCl, 200 mM NaCl, 20 mM $MgCl_2$, 5 mM TCEP, pH 7.5), passed through tandem NiNTA-benzamidine columns and finally through an S200 gel filtration column. Typical yields were 30-40 mg TPX2/L cell culture.

TEV-cleavable, His_6-tagged monobodies were purified from both soluble and insoluble fractions. Monobodies were grown in TB at 37 °C at a starting OD = 0.2. At an OD = 0.6-0.8, cells were induced with 0.6 mM IPTG at 18 °C for 13-15 hours. Cells were centrifuged, resuspended in binding buffer (50 mM TrisHCl, 300 mM NaCl, 20 mM $MgCl_2$, 20 mM imidazole, 10% glycerol, pH 8.0) in the presence of lysozyme, DNase and EDTA-free protease inhibitor cocktail, sonicated, spun down and supernatant was run through a NiNTA column after filtration using a 0.22 μm filtering unit. The pellet thus obtained was resuspended in GuHCl buffer (20 mM TrisHCl, 6 M GuHCl, pH 8.0), placed on a wheel at RT for 10 min and spun down again. The supernatant was filtered through a 0.22 μm filtering unit and run through the NiNTA column previously loaded with the soluble fraction of monobody and pre-equilibrated in GuHCl buffer. In-column monobody refolding was achieved by washing the NiNTA column with 10 column volumes of GuHCl buffer, triton-X buffer (binding buffer + 0.1% Triton X-100), β-cyclodextrin buffer (binding buffer + 5 mM β-cyclodextrin), and finally binding buffer. Monobodies were eluted in 100% elution buffer (binding buffer + 500 mM imidazole) and placed in dialysis cassettes in presence of TEV protease and dialyzed against gel filtration buffer (20 mM TrisHCl, 200 mM NaCl, 20 mM $MgCl_2$, 5 mM TCEP, 10% glycerol, pH 7.5). The

following morning, TEV-cleaved monobodies were placed through a NiNTA column (to remove the His_6 tag, His_6-tagged TEV protease and any residual, uncleaved monobodies), and ran through a 26/60 S200 gel filtration column. Typical yields varied depending on the monobody being purified, but in general were in the 10-30 mg monobody/L cell culture. Monobody sequences are shown in **Fig. 1D**.

Isothermal Titration Calorimetry

All titrations were carried out using the NanoITC (TA instruments) at 25 °C and were comprised of addition of 1 μL injectant every 180 sec, while the solution in the cell was stirred at 350 rpm. Prior to every titration, proteins were dialyzed in ITC buffer (20 mM TrisHCl, 200 mM NaCl, 20 mM $MgCl_2$, 10% glycerol, 1 mM TCEP, pH 7.5) at 4 °C and filtered using SpinX filter columns (Corning). The starting protein concentrations for the runs in **SI Appendix, Fig. S1B** and **Fig. 2** were:

25 μM AurA Y199K (cell) + 1000 μM TPX2 (syringe),
25 μM AurA Y199H (cell) + 1000 μM TPX2 (syringe),
80 μM AurA (cell) + 940 μM TPX2 (syringe),
13 μM AurA (cell) + 98 μM Mb1 (syringe),
32 μM AurA (cell) + 218 μM Mb2 (syringe),
25 μM AurA (cell) + 213 μM Mb3 (syringe),
27 μM AurA (cell) + 242 μM Mb4 (syringe),
11 μM AurA (cell) + 75 μM Mb5 (syringe),
25 μM AurA (cell) + 250 μM Mb6 (syringe).

All titrations were analyzed via the NanoAnalyze software using the independent fit model. In all cases, AurA:monobody ratio was kept around 1:7-1:10.

For ITCs shown in **SI Appendix, Fig. S2**, AurB ITC buffer (31.7 mM HEPES pH 7.3, 317 mM ammonium acetate, 3.8 mM TCEP, 0.63 mM $MgCl_2$, 0.75 M sucrose) was used. The rest of the experimental setup and data analysis were the same. Starting protein concentrations for the runs in **SI Appendix, Fig. S2** were:

27 μM AurB (cell) + 173 μM Mb1 (syringe),
25 μM AurB (cell) + 800 μM Mb1 (syringe),
26 μM AurB (cell) + 190 μM Mb2 (syringe),

21 μM AurB (cell) + 680 μM Mb2 (syringe).

In vitro kinase assays

Kinetic parameters for AurA, such as K_M^{ATP}, K_M^{Lats2}, k_{obs}^{ATP} and k_{obs}^{Lats2} in the presence or absence of TPX2/monobodies, were assessed through the ADP/NADH coupled assay which relates peptide phosphorylation (as measured through ADP production) to the oxidation of NADH to NAD^+. A 96-well microplate reader was used (SpectraMax) and assays were performed in a white, clear-bottom, half-well 96-well plate (Corning #3994) in a final reaction volume of 100 μL per well.

Assays were performed at 25 °C in assay buffer (20 mM TrisHCl, 200 mM NaCl, 20 mM $MgCl_2$, 5 mM TCEP, 10% glycerol, pH 7.5) supplemented with 6.6 mM phosphoenolpyruvate (PEP), 725 μM NADH, 370 nM pyruvate kinase (PK), 350 nM lactate dehydrogenase (LDH), and 0.6 mg/mL BSA. Oxidation of NADH was monitored at A_{340} for 20 min using SOFTmaxPRO software and calculated using the following equation:

$$k_{obs}\,(s^{-1}) = \frac{-dA_{340}}{dt}\,(OD\,s^{-1}) \times K_{path}^{-1}\,(\mu M\,OD^{-1}) \times [enzyme]^{-1}\,(\mu M^{-1})$$

where K_{path} is the molar absorption coefficient for NADH. For a 100 μL well volume, the change in optical path length was experimentally determined to be $K_{path} = 0.0038$ OD/μM. Appropriate controls (ensuring PEP/NADH/PK/LDH are not limiting factors) were carried out before data was gathered.

Lats2 peptide (ATLARRD**S**LQKPGLE) was obtained through Genscript while AurA, TPX2, monobodies were expressed and purified as described above. AurA phosphorylates Lats2, a physiological substrate of the kinase, on a Ser residue (bolded, above). K_M^{Lats2} and k_{obs}^{Lats2} were initially measured for 1 μM AurA in the presence of increasing amounts of peptide (0, 0.2, 0.5, 1, 2, 3, 5, 10, 20 and 30 mM Lats2). In experiments with activating TPX2 / monobodies, less AurA was used to avoid reaction completion during the dead time of the instruments (0.25 μM AurA and 50 μM TPX2 or 0.25 μM AurA and 10 μM Mb1). The other AurA / monobody concentrations used were: 1 μM AurA and 70 μM Mb2, 1 μM AurA and 50 μM Mb3, 1 μM AurA and 10 μM Mb4,

1 μM AurA and 2 μM Mb5, 1 μM AurA and 50 μM Mb6.

For High Performance Liquid Chromatography (HPLC) assays, an Agilent Infinity 1260 system equipped with a high-precision autosampler (injection error <0.1 μL) and an analytical HPLC column (ACE 5 C18-AR column, 2.4 mm i.d., 250 mm length, 5-Å particle size, 100 Å pore size), was used to separate Lats2 species at various reaction time points. For each time point, 5 μL of the reaction mixture was quenched with 10 μL of 6% (vol/vol) trichloroacetic acid in water, spun down using Spin-X centrifugal tube filters (Costar) and then neutralized with 50 μL of 100 mM KH_2PO_4, pH 8.0. Lats2 species were separated using the following program:

- 0-2 min: equilibration in buffer A
- 2-6 min: 0-11.8% buffer B
- 6-7.5 min: 11.8-14.8% buffer B
- 7.5-15 min: 14.8-18.8% buffer B
- 15-16 min: 18.8-100% buffer B
- 16-20 min: 100% buffer B
- 20-25 min: 0% buffer B, re-equilibration with buffer A and preparation for the next autosampler run,

where buffer A = 0.1% trifluoroacetic acid (TFA) in water and buffer B = HPLC-grade acetonitrile. Each run was 25 mins long and the flow rate was kept constant at 0.4 mL/min. Representative HPLC traces are shown in **SI Appendix Fig. S3B** with quantified product shown in the inset and a comparison of rates obtained through the HPLC and ADP/NADH coupled assays shown in **SI Appendix Fig. S3C**. Given the direct translation of peptide phosphorylation to ADP production/NADH oxidation as well as the speed of the coupled assay vs the HPLC assay (96 time points can be run in 20 mins as opposed to 1 time point needing 25 mins to be completed with the HPLC assay), the ADP/NADH coupled assay was routinely preferred over the HPLC assay.

Crystallographic methods

Prior to crystallization, AurA and monobodies were aliquoted in storage buffer (20 mM TrisHCl, 200 mM NaCl, 10% (v/v) glycerol, 20 mM $MgCl_2$, 5 mM TCEP, pH 7.5)

and kept at -80 °C. AMPPCP was prepared fresh from powder the day of crystallization in concentrations of 100-120 mM in storage buffer.

Crystals of AurA in complex with AMPPCP and activating monobody, Mb1, were obtained by combining 0.5 μL of [300 μM AurA + 5 mM AMPPCP + 300 μM Mb1] with 0.5 μL of mother liquor (0.1 M MES sodium salt pH 6.5, 0.2 M ammonium sulfate, 4% (v/v) 1,3-propanediol, 30% (w/v) PEG8000). Crystals were grown at 18 °C by vapor diffusion and the sitting drop method. Crystals were washed with mother liquor and flash frozen in liquid nitrogen in preparation for data collection.

Similarly, crystals of AurA in complex with AMPPCP and inhibiting monobody, Mb2, were grown at 18 °C by vapor diffusion and the sitting drop method. A 1:1 ratio of protein mixture: mother liquor was obtained by combining 0.5 μL of [240 μM AurA + 2.5 mM AMPPCP + 250 μM Mb2] with 0.5 μL of mother liquor (0.1 M Bis-Tris pH 5.5, 0.2 M NaCl, 25 (w/v) PEG 3350). Crystals were flash frozen in liquid nitrogen prior to shipping.

Diffraction data were collected at 100 K at Advanced Light Source (Lawrence Berkeley National Laboratory) beamlines 8.2.2 (Mb1 structure) and the Stanford Synchrotron Radiation Lightsource beamline 7-1 (Mb2 structure) with wavelengths of 1.00 Å (Mb1 structure) and 0.98 Å (Mb2 structure). Data were processed with the automated data reduction program XIA2 [6] that is part of the CCP4-suite [7] and uses AIMLESS, DIALS, DISTL, LABELIT and POINTLESS [8-10]. Initial phases were obtained by molecular replacement (CCP4 programs MOLREP [11] and PHASER [12]) by using an Aurora A kinase structure (PDB ID 4C3R [5]) and a monobody structure (PDB ID 3K2M [2]) as a search model. The refinement was carried out with REFMAC5 [13] and PHENIX.REFINE [14], followed by manual rebuilding in COOT [15, 16].

Ramachandran statistics were calculated using the SFCHECK program in CCP4 [17]. In the 2.06 Å structure of AurA-Mb1-AMPPCP (PDB ID 5G15), the distribution of residues in the favored, allowed and outlier regions of the Ramachandran plot were 96.6%, 3.4% and 0.0%, respectively. Whereas, in the 2.55 Å structure of AurA-Mb2-AMPPCP (PDB ID 6C83), the distribution of residues in the favored, allowed and outlier regions of the Ramachandran plot were 95.2%, 4.6% and 0.2%, respectively.

Residues in AurA directly involved in the binding interface with Mb1, Mb2 or TPX2 (**Fig. 5B, SI Appendix Fig. S4C**) were identified using the PISA software [18].

In order to maintain correspondence between the X-ray structures (PDB IDs 5G15 and 6C83) and constructs shown in the paper, we adopted the convention that the first amino acid in any construct shown is labeled 1, acknowledging that in the monobody constructs the first two amino acids (GS) are a result from BamHI cloning and in other resources may commonly be referred to as -2 and -1.

Analytical Ultracentrifugation

Beckman Optima XL-A Analytical Ultracentrifuge was used to perform sedimentation velocity runs at 50,000 rpm and 18 °C (to match the crystallization temperature). Prior to each run, AurA and monobodies were dialyzed in storage buffer (20 mM TrisHCl, 200 mM NaCl, 10% (v/v) glycerol, 20 mM $MgCl_2$, 5 mM TCEP, pH 7.5) at 4 °C. Sedimentation of 100 μM AurA, 100 μM AurA + 150 μM Mb1 / Mb2 / Mb3 / Mb4 / Mb5 / Mb6 were followed at three different wavelengths (285 nm, 290 nm and 295 nm) for 12 hours. Data were analyzed using the SEDFIT software [19, 20] and the continuous size-distribution option.

SUPPLEMENTARY FIGURES

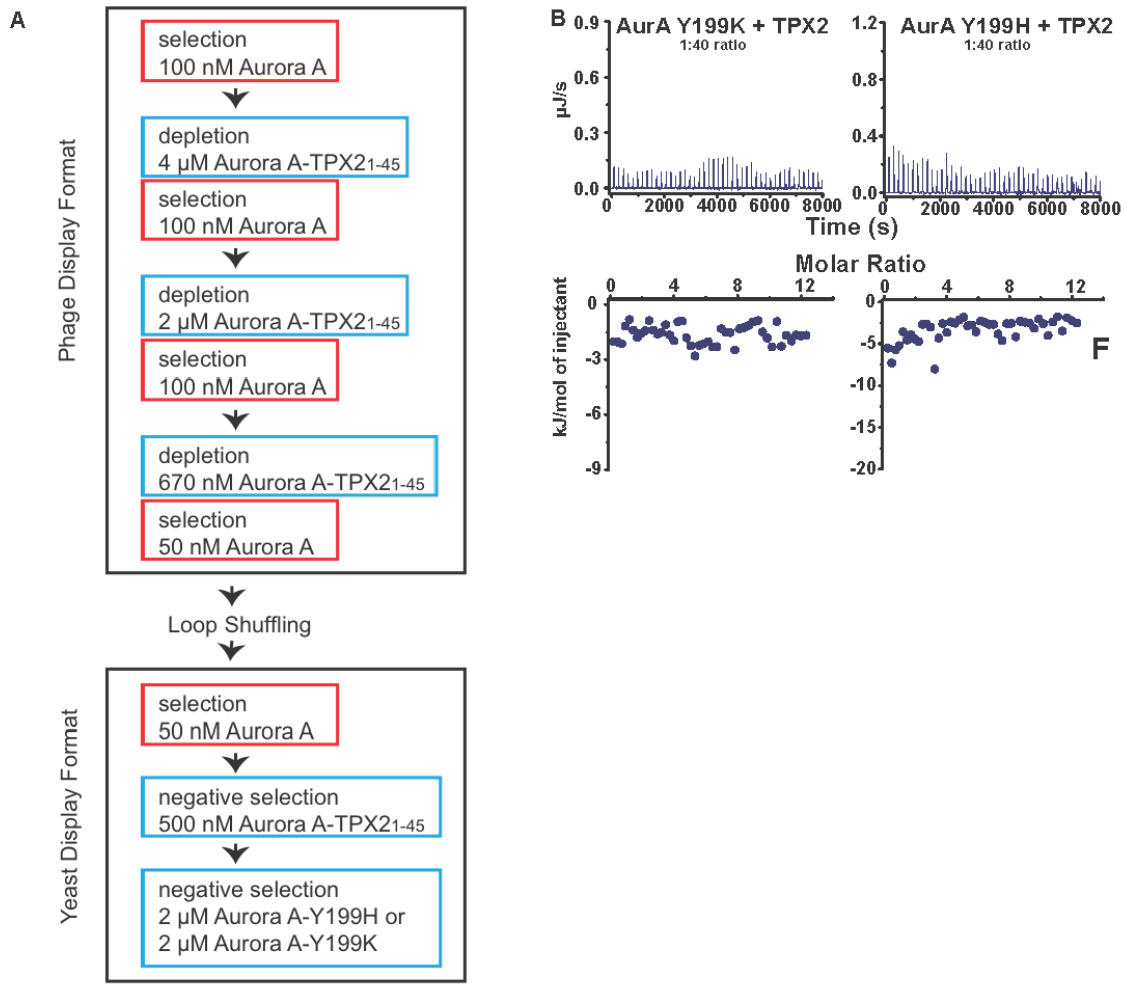

Fig. S1. | **A.** Flow chart showing the monobody selection strategy. In the phage display selection phase, negative selection (depletion) using the AurA-TPX2 fusion was performed prior to positive selection using WT AurA, except for the first round. In yeast display library sorting, one round each of positive selection with WT AurA and negative selection with AurA-TPX2 fusion were performed, followed by one round of negative selection using Y199H and Y199K AurA. **B.** Mutation of AurA Y199 to either H or K leads to severe weakening of TPX2 binding (ITC thermogram of TPX2 binding to WT AurA is shown in **Fig. 2**).

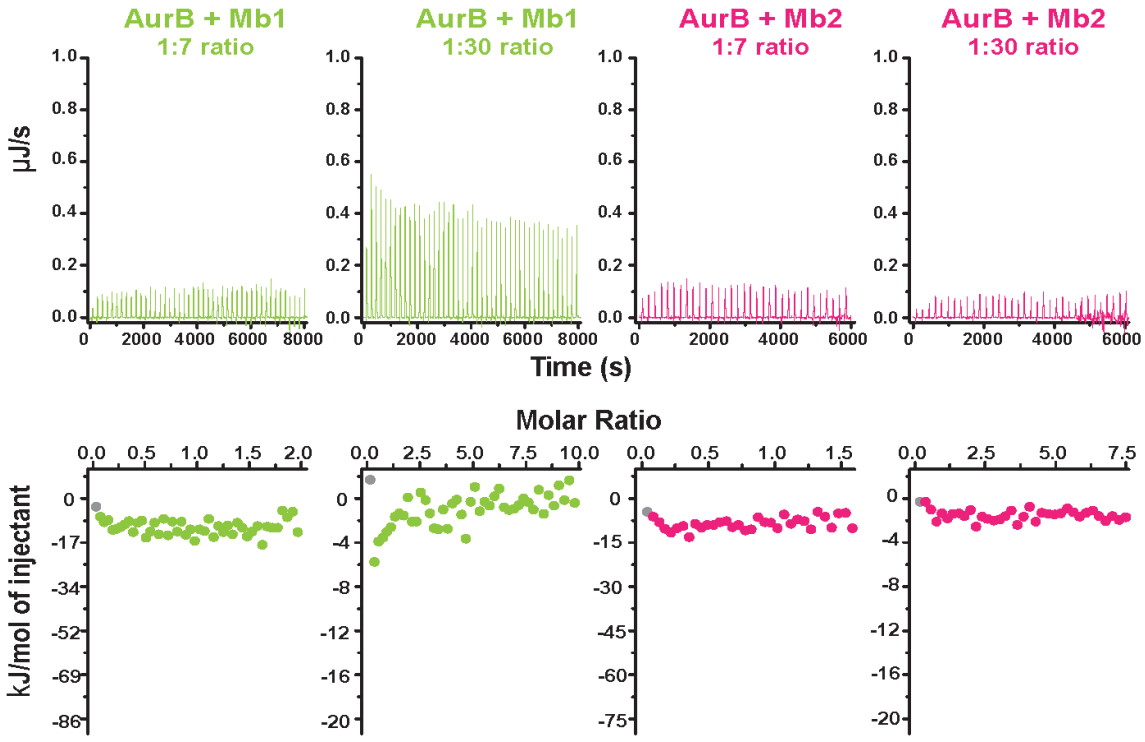

Fig. S2. | AurB, the closest homologue of AurA (74.2% sequence identity) displays no measurable binding to Mb1 and Mb2, the most thoroughly characterized monobodies. Two AurB:Mb protein concentration ratios were used to ensure sampling of a large range of binding affinities. (going from left to right, concentrations used were: 27 µM AurB and 173 µM Mb1, 25 µM AurB and 800 µM Mb1, 26 µM AurB and 190 µM Mb2, 21 µM AurB and 680 µM Mb2)

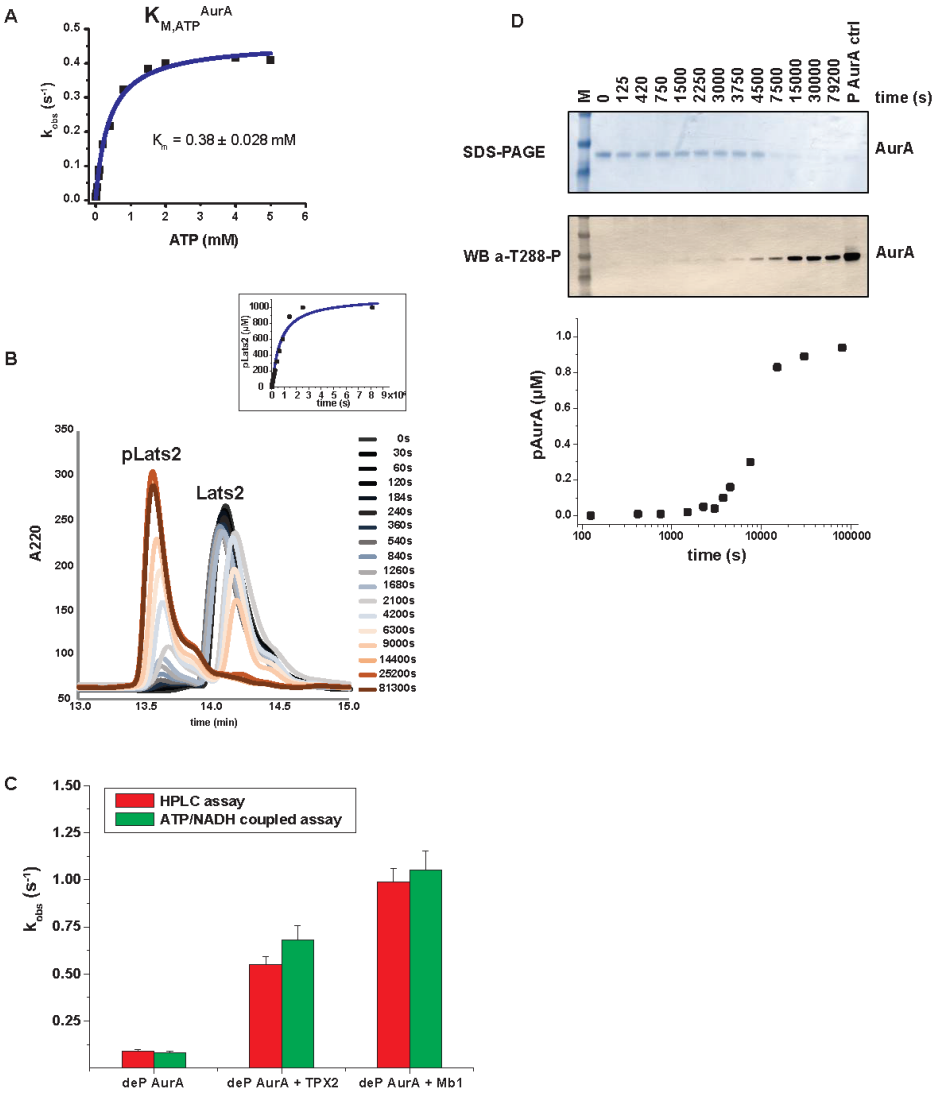

Fig. S3. | Controls for activity assay setup **A.** Michaelis Menten curve of AurA for ATP, normalized by the enzyme concentration, using the ADP/NADH coupled assay. ATP is used at saturating concentrations (5 mM) throughout this work. **B.** Time-course of Lats2 phosphorylation as monitored through High Performance Liquid Chromatography (HPLC). Clear separation of singly phosphorylated and non-phophorylated Lats2 allows for reliable quantification of the area under the peptide peak (attached inset, upper right corner). **C**. Comparison of AurA kinetics obtained from the HPLC (red) or ADP/NADH coupled assay (green). **D.** Assessing AurA autophosphorylation timescales. Autophosphorylation kinetics of 1 µM AurA at various time points as measured through Western Blot against pT288 AurA (CST #3079) shows a lag-phase of 50 mins followed by a log autophosphorylation phase. To account for AurA's dynamic range, the following dilutions were used: 3x dilution up to 7500s, followed by 10x dilution for later time points. 1 µM phosphorylated AurA, as assessed by Mass Spectrometry, was used as positive control. ADP/NADH coupled assays discussed in the text are followed up to 15min (900s) to ensure AurA remains dephosphorylated.

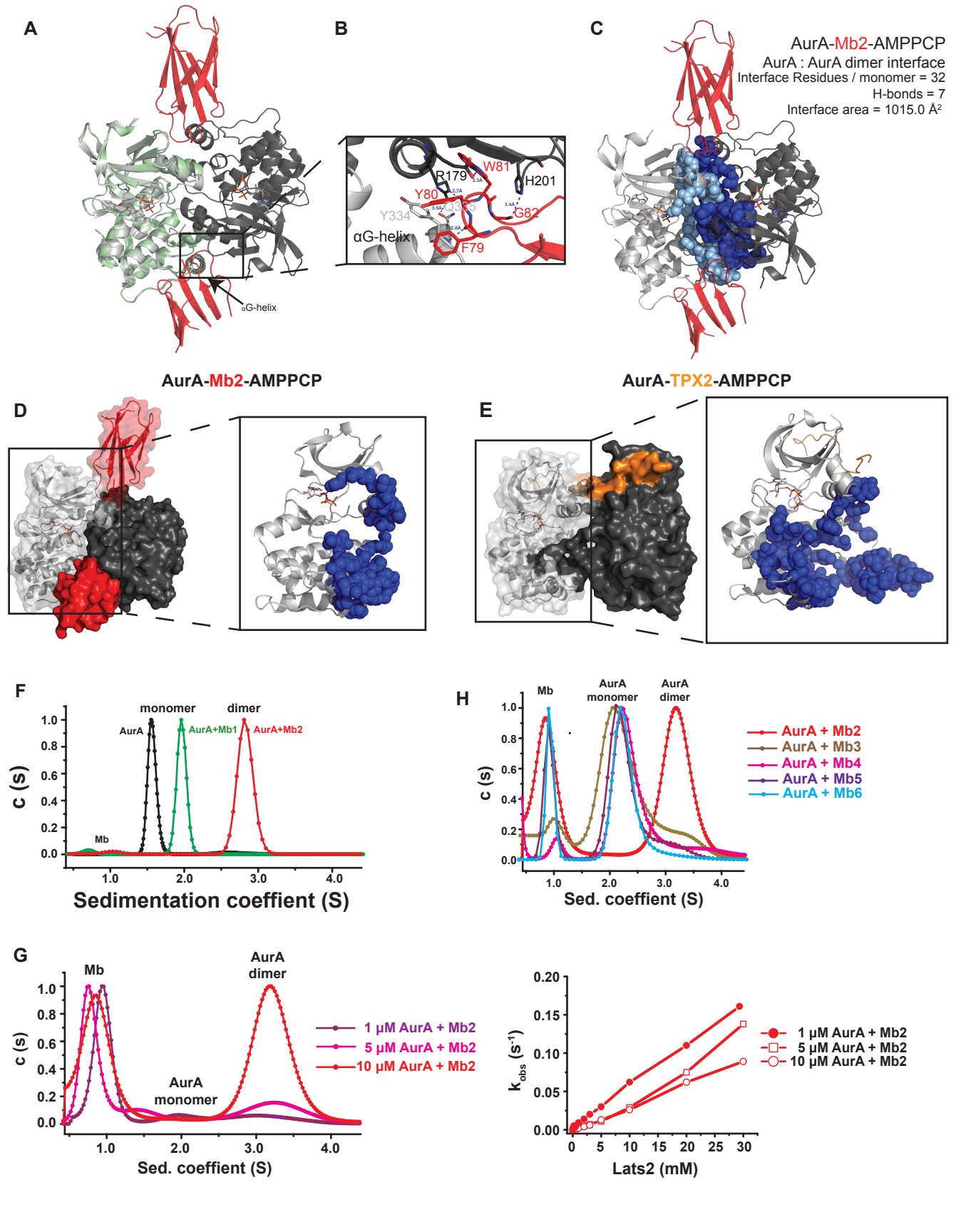
A
αG-helix
B
W81
R179
H201
Y80
Y334
G82
αG-helix
F79
C
AurA-Mb2-AMPPCP
AurA : AurA dimer interface
Interface Residues / monomer = 32
H-bonds = 7
Interface area = 1015.0 Å²
AurA-Mb2-AMPPCP
AurA-TPX2-AMPPCP
D
E
F
monomer
dimer
AurA
AurA+Mb1
AurA+Mb2
Mb
c (s)
Sedimentation coeffient (S)
H
Mb
AurA monomer
AurA dimer
AurA + Mb2
AurA + Mb3
AurA + Mb4
AurA + Mb5
AurA + Mb6
c (s)
Sed. coeffient (S)
G
Mb
AurA dimer
AurA monomer
1 μM AurA + Mb2
5 μM AurA + Mb2
10 μM AurA + Mb2
c (s)
Sed. coeffient (S)
k_obs (s⁻¹)
1 μM AurA + Mb2
5 μM AurA + Mb2
10 μM AurA + Mb2
Lats2 (mM)

Fig. S4. | Dimerization of the AurA-monobody complexes. **A**. Mb2 induced AurA dimerization. Overlay of inactive AurA monomer bound to AMPPCP (green, PDB ID 4C3R) with AurA-Mb2-AMPPCP dimer (PDB ID 6C83) with the two AurA molecules shown in grey and black and Mb2 in red. **B**. Zoom-in into the Mb2-AurA interface illustrates how Mb2 stabilizes the dimerization of AurA via interaction of the monobody with both AurA monomers. H-bonds and salt bridges are shown in blue and green dashed lines, respectively. Several electrostatic and Van der Waals interactions (not shown for clarity) further stabilize this interface. **C**. AurA dimer interface. In the presence of inhibitory monobody Mb2, an extensive AurA : AurA interface is favored (shown in light blue and dark blue spheres). The extent of this interaction is calculated through the PISA analysis reported on the right [18]. **D-E**. Comparison of the AurA-Mb2-AMPPCP dimer **D**. and the AurA-TPX2-AMPPCP dimer (PDB ID 4C3P) **E**. In the AurA-Mb2-AMPPCP dimer, AurA's conformation is very similar to the inactive AurA monomer (PDB ID 4C3R). In contrast, in the AurA-TPX2-AMPPCP dimer, AurA's conformation is very similar to an active AurA monomer. Interface residues for the corresponding dimers are highlighted in blue spheres. **F**. Analytical ultracentrifugation shows that AurA (100 μM) is primarily dimeric in solution in the presence of Mb2 (150 μM) and monomeric when bound to Mb1 (150 μM), supporting the viability of the crystal structures in solution.
G. Dimer formation (left) and corresponding AurA inhibition (right) for AurA : Mb2 as a function of AurA concentrations. 40 μM Mb2 was used in AUC experiments (left) and 70 μM Mb2 were used in activity assays (right). Activity data were normalized by AurA concentrations to report k_{obs}. **H**. Sedimentation velocity AUC data of AurA (20 μM) in the presence of 40 μM inhibitory (Mb3/Mb4/Mb5) and neutral (Mb6) monobodies.

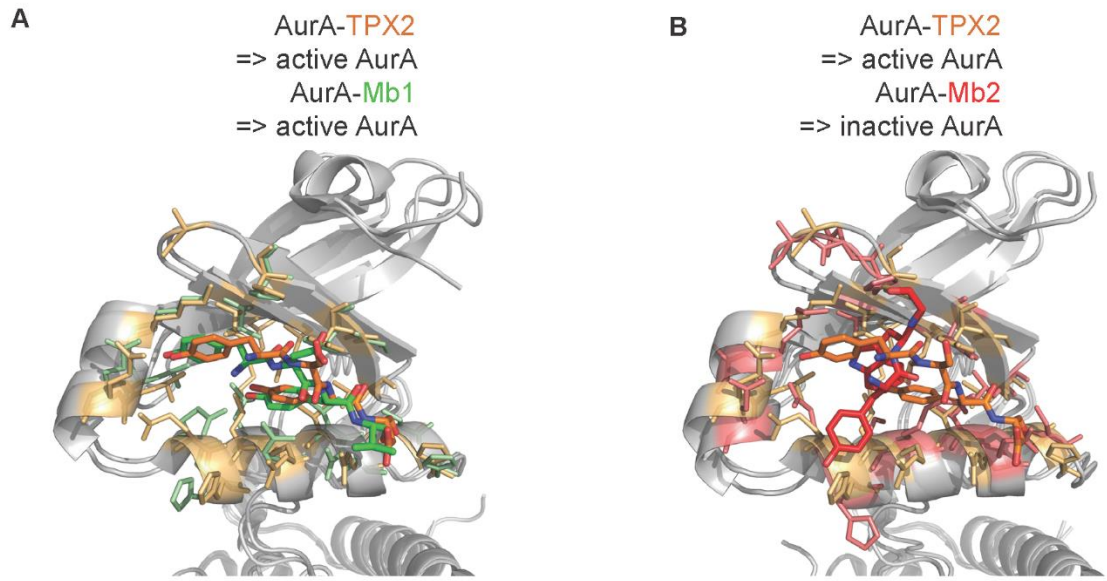

Fig. S5. | Comparison of the binding interface between AurA and TPX2, Mb1 and Mb2. **A**. Superposition of AurA-TPX2 with AurA-Mb1 complex. Interface side-chain conformations are highlighted in the AurA-Mb1 complex in light green for AurA and dark green for Mb1$^{31-35}$, and in the AurA-TPX2 complex in light orange for AurA, and dark orange for TPX2$^{7-11}$. **B**. Superposition of the AurA-TPX2 complex with the AurA-Mb2 complex highlighting interface side-chain residues in pink for the AurA-Mb2 complex and Mb2$^{78-83}$ in dark red.

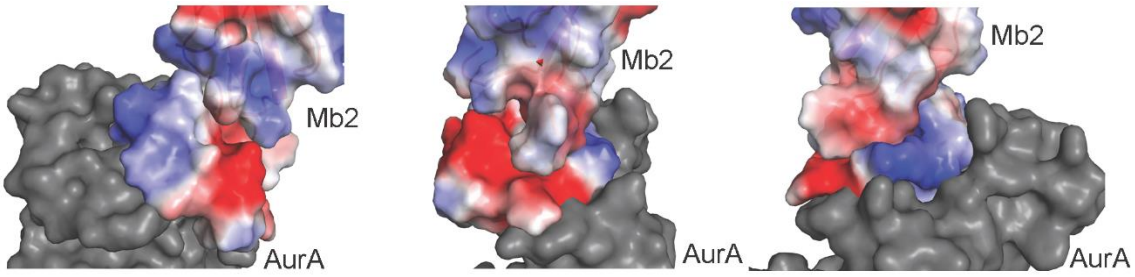

Fig. S6. | Interface between Mb2 and AurA as guide for rational small molecule inhibitor design. Mb2 is shown contacting AurA in three different views (with contacted AurA residues shown in low transparency electrostatic surface rendering and the remainder of AurA in grey). In addition to favorable protein/protein interactions, partially unoccupied pockets are apparent that could be further exploited during small-molecule AurA inhibitor design.

REFERENCE:

1. Koide, A., et al., *Teaching an old scaffold new tricks: monobodies constructed using alternative surfaces of the FN3 scaffold.* J Mol Biol, 2012. **415**(2): p. 393-405.
2. Wojcik, J., et al., *A potent and highly specific FN3 monobody inhibitor of the Abl SH2 domain.* Nat Struct Mol Biol, 2010. **17**(4): p. 519-27.
3. Sha, F., et al., *Dissection of the BCR-ABL signaling network using highly specific monobody inhibitors to the SHP2 SH2 domains.* Proc Natl Acad Sci U S A, 2013. **110**(37): p. 14924-9.
4. Koide, A., et al., *The fibronectin type III domain as a scaffold for novel binding proteins.* J Mol Biol, 1998. **284**(4): p. 1141-51.
5. Zorba, A., et al., *Molecular mechanism of Aurora A kinase autophosphorylation and its allosteric activation by TPX2.* Elife, 2014. **3**: p. e02667.
6. Winter, G., *Xia2: an expert system for macromolecular crystallography data reduction.* J Appl Cryst, 2010(43): p. 186-190.
7. Winn, M.D., et al., *Overview of the CCP4 suite and current developments.* Acta Crystallogr D Biol Crystallogr, 2011. **67**(Pt 4): p. 235-42.
8. Evans, P., *Scaling and assessment of data quality.* Acta Crystallogr D Biol Crystallogr, 2006. **62**(Pt 1): p. 72-82.
9. Sauter, N.K., R.W. Grosse-Kunstleve, and P.D. Adams, *Robust indexing for automatic data collection.* Journal of Applied Crystallography, 2004. **37**(3): p. 399-409.
10. Zhang, Z., et al., *Automated diffraction image analysis and spot searching for high-throughput crystal screening.* Journal of Applied Crystallography, 2006. **39**(1): p. 112-119.
11. Vagin, A.T.A., *MOLREP: an automated program for molecular replacement.* J Appl Cryst, 1997(30): p. 1022-1025.
12. McCoy, A.J., et al., *Phaser crystallographic software.* Journal of Applied Crystallography, 2007. **40**(4): p. 658-674.
13. Murshudov, G.N., et al., *REFMAC5 for the refinement of macromolecular crystal structures.* Acta Crystallogr D Biol Crystallogr, 2011. **67**(Pt 4): p. 355-67.
14. Adams, P.D., et al., *PHENIX: a comprehensive Python-based system for macromolecular structure solution.* Acta Crystallogr D Biol Crystallogr, 2010. **66**(Pt 2): p. 213-21.
15. Emsley, P. and K. Cowtan, *Coot: model-building tools for molecular graphics.* Acta Crystallogr D Biol Crystallogr, 2004. **60**(Pt 12 Pt 1): p. 2126-32.
16. Emsley, P., et al., *Features and development of Coot.* Acta Crystallogr D Biol Crystallogr, 2010. **66**(Pt 4): p. 486-501.
17. Lovell, S.C., et al., *Structure validation by Calpha geometry: phi,psi and Cbeta deviation.* Proteins, 2003. **50**(3): p. 437-50.
18. Krissinel, E. and K. Henrick, *Inference of macromolecular assemblies from crystalline state.* J Mol Biol, 2007. **372**(3): p. 774-97.
19. Dam, J. and P. Schuck, *Calculating sedimentation coefficient distributions by direct modeling of sedimentation velocity concentration profiles.* Methods Enzymol, 2004. **384**: p. 185-212.

20. Schuck, P., *Size-distribution analysis of macromolecules by sedimentation velocity ultracentrifugation and lamm equation modeling.* Biophys J, 2000. **78**(3): p. 1606-19.